CHINESE OPTICS LETTERS

Vol. 20, No. 2 | February 2022

Development of single-resonant optical parametric oscillator with tunable output from 410 nm to 630 nm

Miao Wang (王 淼)[1,2], Jian Ma (马 剑)[1*], Tingting Lu (陆婷婷)[1], Shanjiang Hu (胡善江)[1], Xiaolei Zhu (朱小磊)[1,2,3**], and Weibiao Chen (陈卫标)[1,2,3]

[1] Key Laboratory of Space Laser Communication and Detection Technology, Shanghai Institute of Optics and Fine Mechanics, Chinese Academy of Sciences, Shanghai 201800, China

[2] Center of Materials Science and Optoelectronics Engineering, University of Chinese Academy of Sciences, Beijing 100049, China

[3] Pilot National Laboratory for Marine Science and Technology, Qingdao 266237, China

*Corresponding author: majian@siom.ac.cn

**Corresponding author: xlzhu@siom.ac.cn

Received July 26, 2021 | Accepted August 31, 2021 | Posted Online October 14, 2021

A single-resonant low-threshold type-I β-Ba_2BO_4 (BBO) optical parametric oscillator (OPO) with tunable output from 410 nm to 630 nm at 5 kHz repetition rate is reported. By taking the noncollinear phase matching method, low-threshold OPO operation could be obtained compared with the configuration of collinear phase matching, and the maximum optical–optical conversion efficiency of 11.8% was achieved at 500 nm wavelength when 0.4 mJ pump pulse energy was applied. When the noncollinearity angle was preset at 1.6°, 4.8°, and 6.3°, a continuously tuning output with a total spectral range of 220 nm was successfully obtained by adjusting the phase matching angle of the BBO crystal.

Keywords: optical parametric oscillator; noncollinear phase matching; low threshold; high pulse repetition frequency; widely tunable spectrum range.

DOI: 10.3788/COL202220.021403

1. Introduction

The blue–green spectrum is the optical transmission window of seawater, which can be used for underwater laser communication, laser bathymetry, and ocean LIDAR. The attenuation coefficient varies from different types of seawater, and the optimal wavelengths for laser detection in deep seawater are between 420 nm and 510 nm, while the optimal wavelengths for coastal seawater are between 520 nm and 580 nm[1–5]. As is known[6], an optical parametric oscillator (OPO) pumped by a solid-state laser is regarded as a promising tunable laser source. In particular, a β-Ba_2BO_4 (BBO) OPO pumped by an ultraviolet laser is able to generate a wide range of wavelength emission from blue to near infrared[7–9]. In 1988, Cheng *et al.* firstly, to the best of our knowledge, reported the BBO-OPO pumped by 355 nm with the signal output tunable from 0.48 to 0.63 μm, where its total maximum energy conversion efficiency was 9.4% when the pump pulse energy was ~15 mJ[10]. Later, Fan *et al.* reported a tunable BBO-OPO design, at 30 Hz repetition rate, using three sets of mirrors so that wavelength tuning range covered from 412 nm to 2.55 μm[11].

Recently, a high pulse repetition frequency (PRF) blue–green tunable radiation source with short pulse duration for undersea laser detection has attracted much attention. In 2018, Rao *et al.* reported a 5 kHz nanosecond type-I BBO OPO with maximum output of 3.2 W, which was capable of tuning from 490 nm to 630 nm, and, later in 2021, 1 kHz type-II BBO OPO with tunable output from 500 nm to 600 nm was reported, where the maximum output power was 164 mW[8,12]. In 2021, Binhammer *et al.* reported a high-power quickly tunable noncollinear femtosecond OPO with ultra-broadband output, which is ideally suited for multi-color imaging[13]. In those works, we found that a relatively complex structure and a high pump power were needed. Up to now, there are few reports about miniaturized laser systems for lighting or imaging in seawater applications, which require the characteristics of compact and low-energy consumption.

The cylindrical focusing operation delivers the spot with its minor axis on the walk-off insensitive plane to enhance pump power intensity, and the major axis was set along the walk-off sensitive plane to increase the gain length. Wu *et al.* reported a BBO OPO based on cylindrical focusing of the pump beam to alleviate the influence of walk-off, and, at last, a pump threshold of ~0.4 mJ was achieved[14]. Bosenberg *et al.* reported that the walk-off effect could be compensated by employing two BBO crystals, which are both set to the phase matching angle,

and the walk-off directions are complementary[15]. OPO with a double-pass pumping design also has a lower pump threshold[16,17]. In a noncollinear phase matching design of the BBO OPO pumped by a 355 nm pulse, a large optical conversion efficiency of 40% was obtained due to the pump energy of 28 mJ, which was much beyond the OPO pump threshold energy with a PRF of 10 Hz [18]. It has been proven that the compact design of a noncollinear phase matching OPO is suitable for deep sea application with wide tuning range.

In this paper, a low-threshold type-I single-resonant noncollinear phase matching BBO-OPO was developed, and the total wavelength tunable range is from 410 nm to 630 nm. This laser system employed the structure composed of a home-made 355 nm pump laser and a single plane-plane cavity BBO-OPO unit. The 355 nm pump laser delivered a pulse energy of ~0.4 mJ with a PRF of 5 kHz. Without replacing any devices and mirrors, the signal output spectrum covered a range of 220 nm, while the noncollinearity angles were, respectively, set at 1.6°, 4.8°, and 6.3°. The pulse repetition rate of the signal output laser was 5 kHz with a pulse width of ~1.6 ns. A maximum signal output energy of 48 μJ and a conversion efficiency of 11.8% were achieved, while the pump energy was up to 0.4 mJ. Thus, with the advantages of compact and low-energy consumption, the laser system could be excellently applied to integrate in a small submersible for underwater multi-color imaging.

2. Theory and Design Basis

The energy conversion efficiency of a single-resonant pulsed OPO is defined as[19]

$$\eta = 0.9 \times M \times \frac{(\log N)^{2.33}}{N}, \tag{1}$$

where M is a coefficient related to the reflectivity of the OC and the loss of OPO, and N is the ratio of the pump energy to the pump threshold energy. Equation (1) shows that high conversion efficiency is attributed to a large N value. The pump threshold energy is limited by parametric gain length L, which is defined by

$$L = l_w \times \mathrm{erf}\left(\frac{\sqrt{\pi} \times l}{2 \times l_w}\right), \tag{2}$$

$$l_w = \frac{\sqrt{\pi}}{2} \times \frac{w_p}{\rho} \times \sqrt{\frac{w_p^2 + w_s^2}{w_p^2 + w_s^2/2}}, \tag{3}$$

where l_w is the crystal walk-off length, w_p and w_s are the Gaussian mode electric-field radius, and ρ is the walk-off angle. It is obvious that due to the walk-off angle (~70 mrad) of 355 nm laser caused by the birefringence of the BBO crystal, the pulsed OPO energy conversion efficiency is severely limited.

Figure 1 shows the schematic diagram of the noncollinear phase matching OPO setup. Phase matching is represented by $\boldsymbol{K}_p$, $\boldsymbol{K}_i$, and $\boldsymbol{K}_s$, which satisfies $\boldsymbol{K}_p = \boldsymbol{K}_s + \boldsymbol{K}_i$. The normal direction of the OPO cavity lies in an angle of positive α to the pump wave vector $\boldsymbol{K}_p$. For convenience of description, the angle α is defined as the noncollinearity angle. Under these circumstances, the tangential phase matching (TPM) condition is satisfied, as shown in Fig. 2[18], where ΔK represents the tolerance of phase mismatching. In this situation, a large acceptance angle of 355 nm laser in BBO is obtained so that the pump threshold of the OPO decreased. The finite pump beam divergence would lead to a broadening linewidth of the signal output[18,20]. In another case, by taking a negative noncollinearity angle α, the Poynting vectors of the pump and signal are nearly collinear in the crystal so that the parametric gain length is increased. It is proven that the conditions of TPM and Poynting vector compensation require opposite noncollinearity angle, as Fig. 2 shows. For the reasons of low pump energy, a single lens focused the laser beam into BBO crystal to enhance the power density and produced a large beam divergence so that TPM condition was suitable[21].

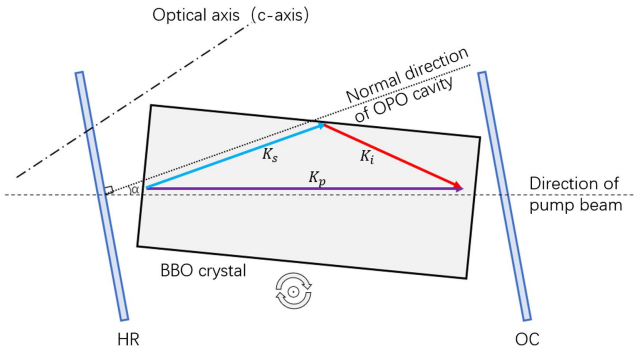

Fig. 1. Schematic diagram of the noncollinear phase matching setup.

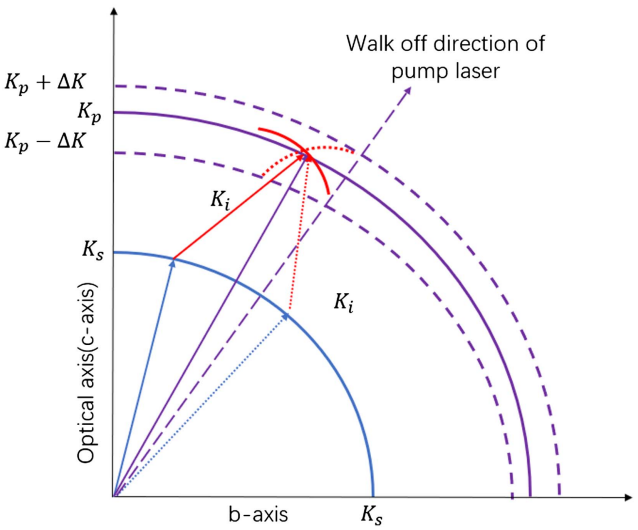

Fig. 2. Phase matching schematic of the TPM condition (solid line) and walk-off compensation condition (dotted line).

3. Experimental Setup

The schematic diagram of the tunable noncollinear phase matching OPO is shown in Fig. 3. The laser system consists of two components, a home-made 355 nm pump laser and a plane-plane cavity BBO-OPO unit.

As Fig. 4(a) shows, the home-made 355 nm pump laser delivered 5 kHz pulsed output. A pulse temporal profile of the 355 nm laser was smooth with a pulse duration of 3.3 ns. M2 was used to change the noncollinearity angle α. Short focal length would lead to a large beam divergence, and long focal length would not provide adequate pump power density. The focal length of the lens was chosen as 205 mm so that the spot size of the pump laser was decreased to 0.7 mm.

A type-I phase matching BBO crystal with dimensions of $8\,\text{mm} \times 8\,\text{mm} \times 20\,\text{mm}$, cut at $\theta = 29.6°$ and $\varphi = 90°$ was inserted in a 35 mm length plane-plane resonator. The BBO crystal was rotated ±3° to generate signal wavelength tunable output. The size of the BBO crystal should ensure that the rotating crystal would not block the path of the pump, signal, and idler. Due to the TPM condition, the gain length in the BBO crystal is not the major factor to influence conversion efficiency, so the crystal size was chosen based on existing conditions. A large cross section and a not very long length were suitable. The plane mirror M3 was high-reflection coated at 430–600 nm and anti-reflection coated at 355 nm and 860–2030 nm, while the plane mirror M4 was anti-reflection coated at 355 nm and 860–2030 nm, with a reflectivity of ~80% at 430–600 nm.

In the experiments, M2 was firstly set at an angle of 45°, and the BBO crystal was aligned to the pump beam, while the angle between the normal direction of the OPO resonator and pump beam direction was $\alpha_1 = 1.6°$. By employing an auxiliary visible laser behind M1 with the laser beam overlapped with the pump laser, the spot of the auxiliary visible laser had a displacement at the position of the block plane, as Fig. 3 shows. The radiation direction of signal output was settled due to the fixed OPO resonance when the angle of M2 was changed. The signal, idler, and residual pump beam were separated spatially due to noncollinear phase matching. The residual pump laser was blocked, and the signal laser could be output. Another two angles $\alpha_2 = 4.8°$ and $\alpha_3 = 6.3°$ were chosen to broaden the signal output spectrum range. By using a manually adjustable fixture to hold the BBO crystal, rotating operation was achieved.

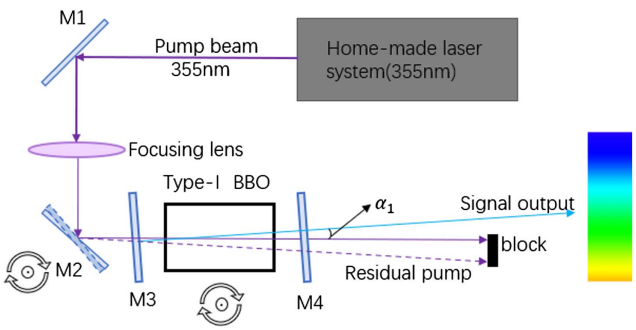

Fig. 3. Schematic diagram of the experimental setup.

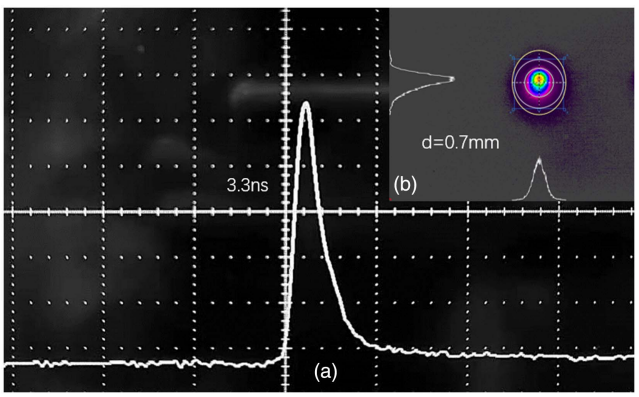

Fig. 4. (a) Pulse temporal profile of the 355 nm laser; (b) spot size of the 355 nm beam at the position of the BBO crystal.

4. Result and Discussion

The home-made Q-switched pump laser offered an average power of 2 W with a pulse duration of 3.3 ns. The beam diameter at the position of the BBO crystal was 0.7 mm, as Fig. 4(b) shows. The 355 nm laser maximum peak power density was around $62\,\text{MW/cm}^2$. Relatively high pump pulse energy threshold of the collinear phase matching BBO-OPO is the major difficulty to achieve high repetition rate widely tunable output. The peak power density mentioned above did not reach the OPO threshold while taking the collinear phase matching configuration (about $\sim 140\,\text{MW/cm}^2$ in theory).

A maximum signal output average power of 240 mW has been generated with the 355 nm pump power of 2 W, corresponding to a conversion efficiency of 11.8% at 500 nm, while taking $\alpha_2 = 4.8°$. As Fig. 5 shows, the pulse duration of the signal output laser at 500 nm was about 1.6 ns. Another two noncollinearity angles ($\alpha_1 = 1.6°$ and $\alpha_3 = 6.3°$) have been taken to broaden the tunable spectrum range. Figure 6 shows the output spectrum

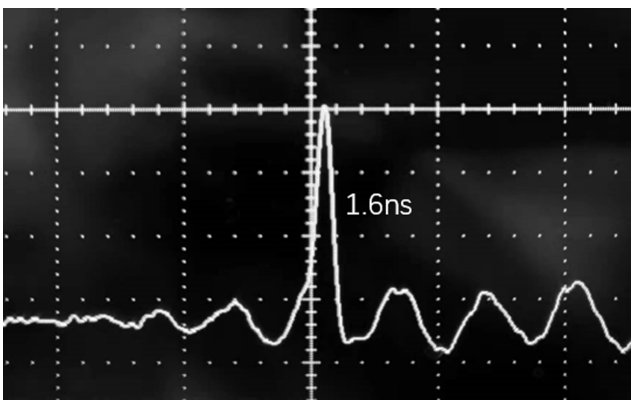

Fig. 5. Pulse temporal profile of the signal output at 500 nm.

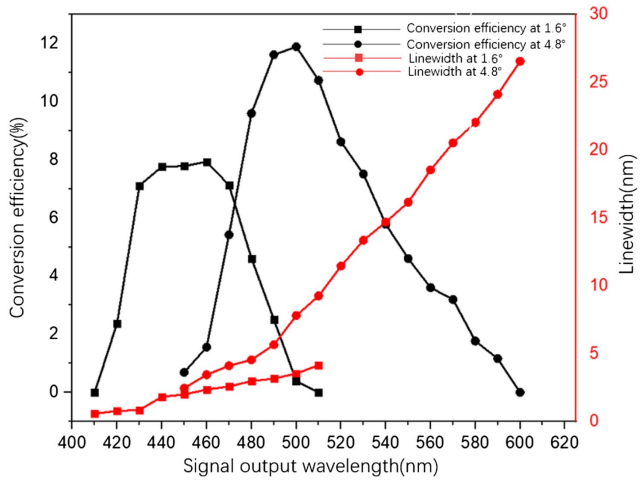

Fig. 6. Signal linewidth and conversion efficiency varying with wavelength at α_1 =1.6° and α_2 = 4.8°.

characteristics when taking $\alpha_2 = 4.8°$. It can be seen that the linewidth became broader when the signal wavelength was tuning to red because of the approaching degeneracy point and the increasing of gain bandwidth. Besides, due to pump beam divergence, gain linewidth, noncollinearity angle, and parametric gain process itself, the linewidth of signal output is much larger than that using collinear phase matching. It is proven that the TPM condition introduces a broader linewidth than conditions of collinear phase matching[18,21].

The noncollinearity angle was settled when the BBO crystal was rotating around the geometric axis (*a* axis). When the noncollinearity angle was set at 1.6°, 4.8°, and 6.3°, the spectrum range was obtained at 410–510 nm, 440–600 nm, and 470–630 nm, respectively. Figure 7 shows that the widely tunable signal laser outputs vary with different noncollinearity angles. An overall continuously tuning spectrum from 410 nm to 630 nm was achieved.

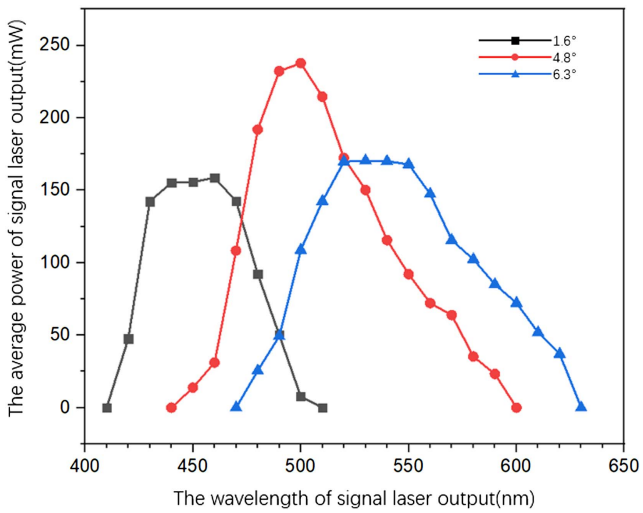

Fig. 7. Widely tunable signal laser outputs vary with different non-collinearity angles.

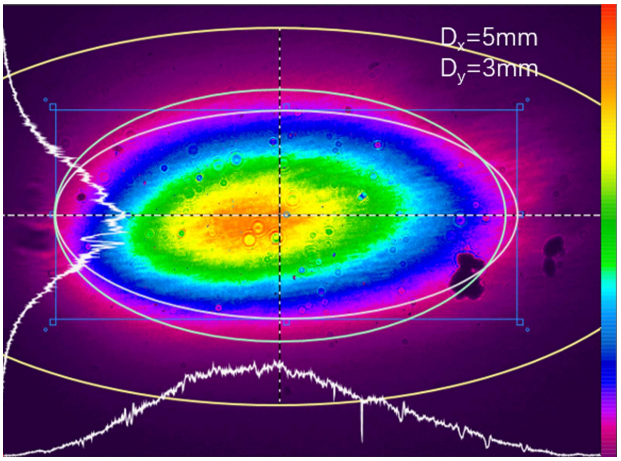

Fig. 8. Beam profile of the signal output at 500 nm.

Figure 8 shows the beam profile of the output signal laser, where the major and minor axes were 5 mm and 3 mm long respectively at the position of 360 mm away from the output coupler. The far-field divergence angle of output laser was 7.0 mrad in the *x* direction and 4.6 mrad in the *y* direction.

5. Conclusion

In conclusion, adopting a noncollinear phase matching configuration, a compact low-threshold BBO-OPO with wide tunability in the blue–green–yellow spectral range has been developed. With the noncollinearity angle preset at 4.8°, a maximum output signal pulse energy of 48 μJ at 500 nm was obtained, while 0.4 mJ of 355 nm pump pulse energy was applied; by presetting the noncollinearity angle at 1.6°, 4.8°, and 6.3°, a continuously tunable output from 410 nm to 630 nm was achieved.

Acknowledgement

This work was supported by the Natural Science Foundation of Shanghai (No. 19YF1453600), the Key Task Project in Scientific and Technological Research on Social Development of Shanghai (No. 20dz1206502), the Marine S&T Fund of Shandong Province for Pilot National Laboratory for Marine Science and Technology (Qingdao) (No. 2018SDKJ0102), the Strategic Priority Research Program of the Chinese Academy of Sciences (No. XDA22000000), and the Major Program of the National Natural Science Foundation of China (No. 61991453).

References

1. J. Zhang, J. Ma, T. Lu, D. Liu, X. Zhu, and W. Chen, "Compact wavelength tunable output around 440 nm pulsed laser for oceanic lidar application," Opt. Commun. **485**, 126706 (2021).
2. S. A. Sullivan, "Experimental study of the absorption in distilled water, artificial sea water, and heavy water in the visible region of the spectrum," J. Opt. Soc. Am. **53**, 962 (1963).

3. A. Morel, B. Gentili, H. Claustre, M. Babin, A. Bricaud, J. Ras, and F. Tièche, "Optical properties of the "clearest" natural waters," Limnol. Oceanorg. **52**, 217 (2007).
4. Y. Zhang, J. Zou, W. Zheng, K. Feng, B. Xu, and Z. Yu, "Watt-level continuous-wave intracavity frequency-doubled Pr:YLF-LBO laser at 320 nm," Chin. Opt. Lett. **19**, 091406 (2021).
5. L. Zeng, X. Sun, Z. Chang, Y. Hu, and J. Duan, "Tunable phase-shifted fiber Bragg grating based on a microchannel fabricated by a femtosecond laser," Chin. Opt. Lett. **19**, 030602 (2021).
6. R. C. Bapna, C. S. Rao, and K. Dasgupta, "Low-threshold operation of a 355-nm pumped nanosecond β-BaB_2O_4 optical parametric oscillator," Opt. Laser. Technol. **40**, 832 (2008).
7. A. Fix, T. Schröder, R. Wallenstein, J. B. Haub, M. J. Johnson, and B. J. Orr, "Tunable γ-barium borate optical parametric oscillator: operating characteristics with and without injection seeding," J. Opt. Soc. Am. B **10**, 1744 (1993).
8. C. S. Rao, S. Kundu, and A. K. Ray, "High repetition rate nanosecond optical parametric oscillator pumped by the third harmonic of a DPSSL," Appl. Phys. B **124**, 163 (2018).
9. J. Ma, T. Lu, X. Zhu, X. Ma, S. Li, T. Zhou, and W. Chen, "Highly efficient H-β Fraunhofer line optical parametric oscillator pumped by a single-frequency 355 nm laser," Chin. Opt. Lett. **16**, 081901 (2018).
10. L. K. Cheng, W. R. Bosenberg, and C. L. Tang, "Broadly tunable optical parametric oscillation in β-Ba_2BO_4," Appl. Phys. Lett. **53**, 175 (1988).
11. Y. X. Fan, R. C. Eckardt, R. L. Byer, J. Nolting, and R. Wallenstein, "Visible Ba_2BO_4 optical parametric oscillator pumped at 355 nm by a single-axial-mode pulsed source," Appl. Phys. Lett. **53**, 2014 (1988).
12. C. S. Rao, S. Kundu, and A. K. Ray, "SLM operation of a high repetition rate BBO optical parametric oscillator pumped by DPSSL at 355 nm," Opt. Laser. Technol. **138**, 106878 (2021).
13. Y. Binhammer, T. Binhammer, R. Mevert, T. Lang, A. Rück, and U. Morgner, "Fast-tunable femtosecond visible radiation via sum-frequency generation from a high power NIR NOPO," Opt. Express **29**, 22366 (2021).
14. S. Wu, G. A. Blake, S. Sun, and J. Ling, "Low-threshold BBO OPO with cylindrical focusing," Proc. SPIE **3263**, 308346 (1998).
15. W. Bosenberg, W. Pelouch, and C. L. Tang, "High-efficiency and narrow-linewidth operation of a two-crystal BaB_2O_4 optical parametric oscillator," Appl. Phys. Lett. **55**, 1952 (1989).
16. R. Smith, "Optical parametric oscillators," Lasers **4**, 189 (1976).
17. Y. Wang, Z. Xu, D. Deng, W. Zheng, X. Liu, B. Wu, and C. Chen, "Highly efficient visible and infrared β-BaB_2O_4 optical parametric oscillator with pump reflection," Appl. Phys. Lett. **58**, 1461 (1991).
18. L. A. W. Gloster, Z. X. Jiang, and T. A. King, "Characterization of an Nd:YAG-pumped β-BaB_2O_4 optical parametric oscillator in collinear and noncollinear phase-matched configurations," IEEE J. Quantum. Electron. **30**, 2961 (1994).
19. E. Granot, S. Pearl, and M. M. Tilleman, "Analytical solution for a lossy singly resonant optical parametric oscillator," J. Opt. Soc. Am. B **17**, 381 (2000).
20. J. Falk and J. E. Murray, "Single-cavity noncollinear optical parametric oscillation," Appl. Phys. Lett. **14**, 245 (1969).
21. A. L. Oien, I. T. McKinnie, P. Jain, N. A. Russell, D. M. Warrington, and L. A. W. Gloster, "Efficient, low-threshold collinear and noncollinear β-barium borate optical parametric oscillators," Opt. Lett. **22**, 859 (1997).